



Indian Institute of  
Technology Delhi



THE UNIVERSITY  
OF QUEENSLAND  
AUSTRALIA

Investigation of High-Temperature Latent Heat Storage Integrated with  
Supercritical CO<sub>2</sub>  
Brayton Cycle

By

**Alok Kumar Ray**

Submitted

in fulfillment of the requirements for the joint degree of

**DOCTOR OF PHILOSOPHY**

to the

**INDIAN INSTITUTE OF TECHNOLOGY DELHI**

**&**

**THE UNIVERSITY OF QUEENSLAND**

**(June 2023)**



Indian Institute of  
Technology Delhi



THE UNIVERSITY  
OF QUEENSLAND  
AUSTRALIA

Investigation of High-Temperature Latent Heat Storage Integrated with  
Supercritical CO<sub>2</sub>  
Brayton Cycle

By

**Alok Kumar Ray**

Submitted

in fulfillment of the requirements for the joint degree of

**DOCTOR OF PHILOSOPHY**

to the

**INDIAN INSTITUTE OF TECHNOLOGY DELHI**

**&**

**THE UNIVERSITY OF QUEENSLAND**

**(June 2023)**

---

*Dedicated to my family members*

---

---

## *Supervisor Certification*

---

This is to certify that the thesis entitled “**Investigation of High-Temperature Latent Heat Storage Integrated with Supercritical CO<sub>2</sub> Brayton Cycle**” being submitted by **Mr. Alok Kumar Ray** to the **Indian Institute of Technology Delhi, India, and The University of Queensland, Australia**, for the award of the degree of ‘**Doctor of Philosophy**’ is a record of the bonafide research work carried out by him. Mr. Alok Kumar Ray has worked under our guidance and fulfilled the requirements for submitting this thesis, which has reached the requisite standard to our knowledge. The results in the thesis are original and have not been submitted, in part or full, to any other University or Institute to award any degree or diploma.

**Prof. Hal Gurgenci**

Emeritus Professor  
School of Mechanical and  
Mining Engineering,

The University of Queensland  
St. Lucia, Australia - 4076

**Dr. Dibakar Rakshit**

Associate Professor  
Department of Energy  
Science and Engineering

Indian Institute of  
Technology Delhi  
Hauz Khas New Delhi, India -  
110016

**Dr. K. Ravi Kumar**

Associate Professor  
Department of Energy  
Science and Engineering

Indian Institute of  
Technology Delhi  
Hauz Khas New Delhi, India -  
110016

---

## Abstract

---

The ever-increasing demand for energy and concern for environmental security has attracted considerable attention from researchers from fossil fuel technology towards renewable energy technology (e.g., solar energy, wind energy, etc.) and variable energy resources. Variable energy sources (e.g., Concentrating solar thermal systems, electricity spillage from PV and wind plants) can play significant roles in the complete transition to renewable energy resources. However, spatial and temporal intermittency is the major hindrance to the effective deployment of renewable energy technologies. Integrating thermal energy storage (TES) systems with renewable energy technologies can reduce the discrepancy between energy supply and demand, leading to continuous energy supply. However, the technologies need to evolve at higher operating temperatures (Thermal stability  $> 550^{\circ}\text{C}$ ) to enable the deployment of efficient thermodynamic cycles such as the supercritical  $\text{CO}_2$  ( $\text{sCO}_2$ ) cycle.

Among the various alternatives of TES technologies, high-temperature latent heat (HT-LHS) storage has significant benefits, such as isothermal operation, high energy storage density, and high exergetic efficiency. Moreover, high-temperature latent heat storage can be integrated with advanced power generation cycles or Thermionic photovoltaic (TIPV) systems to generate cost-effective heat and power. Hence, a critical analysis is imperative to investigate charging and discharging characteristics of the high-temperature latent heat storage. To demonstrate the utility of the HT-LHS system, numerical, theoretical, and experimental studies must be performed.

In this regard, a numerical investigation is conducted to study the thermo-hydraulic behavior during the melting/solidification of high-temperature metallic phase change material (silicon). A counter-clockwise circulation pattern is observed in the molten silicon, unlike clockwise pattern in molten conventional high-temperature PCM (sodium nitrate). The energy storage density and energy storage rates of silicon-based LHS are observed to be significantly higher than sodium nitrate ( $\text{NaNO}_3$ ) based LHS. A suitable high-temperature metallic PCM is identified for HT-LHS system to be integrated with the  $\text{sCO}_2$  Brayton cycle. Steady-state modeling of recompression  $\text{sCO}_2$  Brayton cycle is performed to ascertain the effect of turbine inlet temperature on the thermodynamic efficiency. The thermodynamic efficiency reaches 50% at  $700^{\circ}\text{C}$ , which is significantly higher than the conventional Rankine cycle. The thermal efficiency is maximized at a split ratio of 0.75 for an air temperature of  $30^{\circ}\text{C}$ . Turbine inlet pressure and air

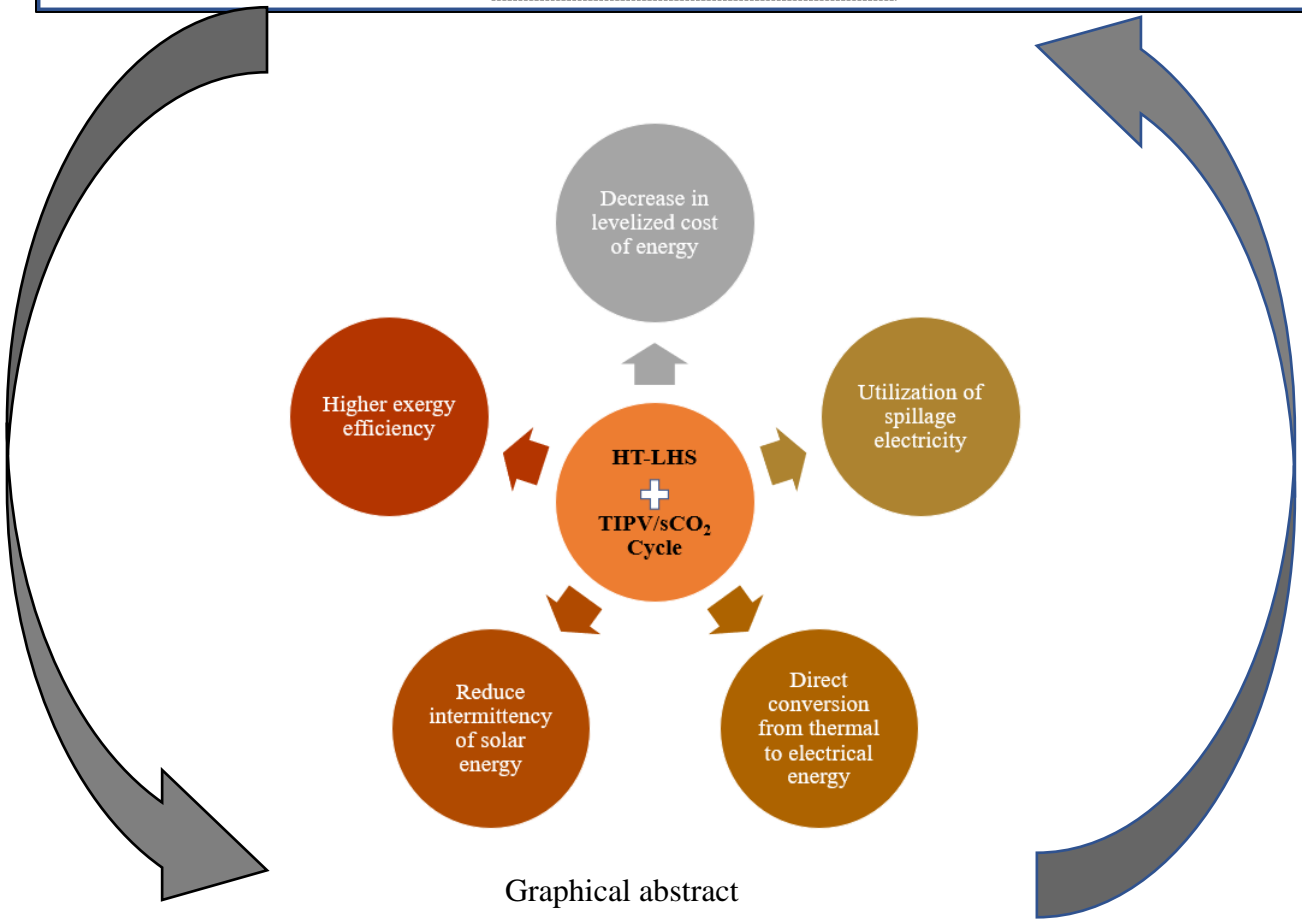
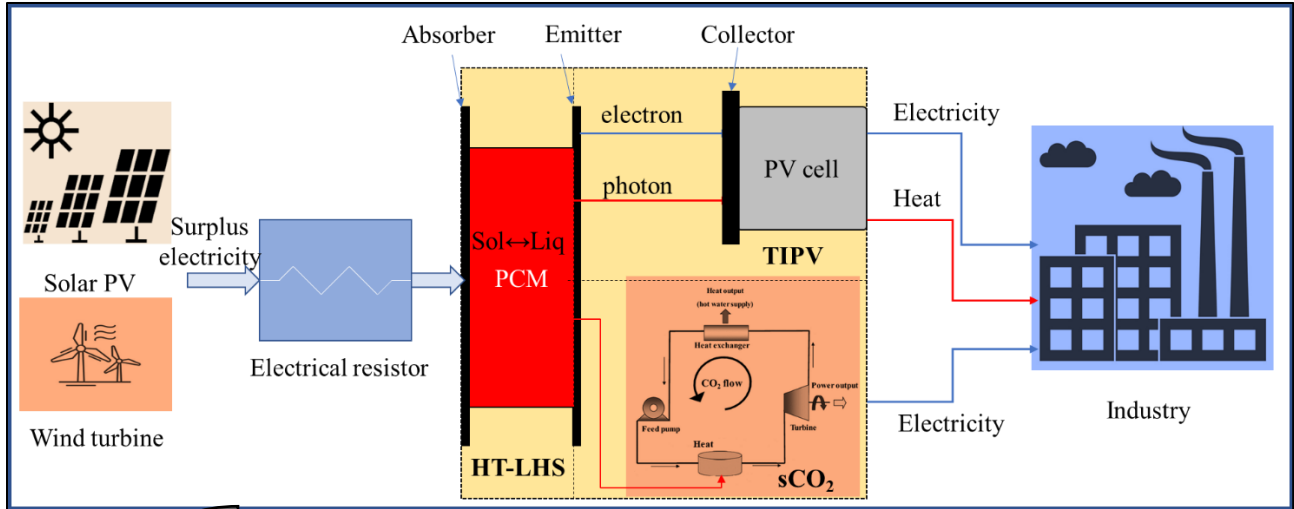
temperature are identified as the most and least sensitive parameters affecting cycle efficiency. A robust analytical model is developed for the discharge operation of the HT-LHS system in dimensionless form and solved to evaluate the discharge performance. Low heat transfer rate is the major technological challenge for HT-LHS systems with conventional inorganic salts. The individual and combined effects of passive heat transfer enhancement methods on the charging and discharging performance of HT-LHS systems are numerically studied. Commercial high-temperature inorganic salt (eutectic mixture of  $\text{NaNO}_3$  and  $\text{KNO}_3$ ) is considered as PCM in the concentric tube storage system. The combined effect on thermal performance is reported to be substantially higher than the individual effect. However, the combined effect of orientation and eccentricity results in a design anomaly for HT-LHS system. Eutectic mixture (60%  $\text{NaNO}_3$ , 40%  $\text{KNO}_3$ ) is synthesized using the common solvent method, and the thermal response of the synthesized sample is studied experimentally. A lab-scale prototype and experimental test facility are designed and developed to mimic the charging and discharging process of a concentric tube HT-LHS system. Moreover, results from the numerical model are validated against the experimental results. To further establish the inevitability of the HT-LHS system, a techno-economic comparative study is conducted between the HT-LHS system and Li-ion battery having the same capacity. The volumetric and gravimetric energy densities are observed to be significantly higher than the Li-ion battery. The charging and discharging durations for HT-LHS system are relatively smaller than the Li-ion battery. The abstract can be graphically depicted in the following Figure.

ऊर्जा की लगातार बढ़ती मांग और पर्यावरण सुरक्षा के चिंता ने फॉसिल ईंधन प्रौद्योगिकी से अधिकर ऊर्जा प्रौद्योगिकी (जैसे कि सौर ऊर्जा, पवन ऊर्जा, आदि) और परिवर्तनशील ऊर्जा संसाधनों की ओर से अध्ययनकर्ताओं को काफी ध्यान आकर्षित किया है। परिवर्तनशील ऊर्जा स्रोतों (जैसे कि संचालक सौर थर्मल प्रणालियाँ, पीवी और पवन प्लांट से बिजली बहाव) में पूरी तरह से आधारभूत ऊर्जा संसाधनों के लिए महत्वपूर्ण भूमिका निभा सकते हैं। हालांकि, स्थानिक और समयिक अनियमितता पर्यावरणीय ऊर्जा प्रौद्योगिकियों के प्रभावी निगमन में मुख्य बाधा है। ऊर्जा परिरक्षण तंत्र (टीईएस) प्रणालियों को ऊर्जा आपूर्ति और मांग के बीच अंतर को कम करके निरंतर ऊर्जा आपूर्ति के मार्ग की प्रमुख बाधाओं को कम करने के लिए परिवर्तनशील ऊर्जा प्रौद्योगिकियों के साथ एकीकृत करने की आवश्यकता होती है। हालांकि, प्रौद्योगिकियों को उच्च संचालन तापमानों (थर्मल स्थिरता  $> 550^{\circ}\text{C}$ ) पर विकसित करने की आवश्यकता होती है ताकि अत्यधिक उष्णमिति आधारित चक्र (सुपरक्रिटिकल सीओ<sub>2</sub> (sCO<sub>2</sub>) चक्र) जैसे कुशल थर्मोडायनामिक चक्रों को विस्तारित करने की संभावना हो।

टीईएस प्रौद्योगिकियों के विभिन्न विकल्पों में उच्च तापमान लटेंट ऊष्मा (एचटी-एलएचएस) संग्रह जैसे महत्वपूर्ण लाभ होते हैं, जैसे कि आइसोथर्मल संचालन, उच्च ऊष्मा संग्रह प्रतिष्ठा, और उच्च प्रदीपादी दक्षता। इसके अलावा, उच्च तापमान लटेंट ऊष्मा संग्रह को उन्नत बिजली प्रजनन चक्रों या थर्माइनिक फोटोवोल्टेक (टीआईपीवी) प्रणालियों के साथ समकालिक ताप और ऊर्जा उत्पन्न करने के लिए एकीकृत किया जा सकता है। इसलिए, उच्च तापमान लटेंट ऊष्मा संग्रह के चार्जिंग और डिस्चार्जिंग गुणधर्मों का विश्लेषण महत्वपूर्ण है। उच्च तापमान लटेंट ऊष्मा संग्रह के गुणधर्मों की प्रदर्शन की प्रतिष्ठ करने के लिए संख्यात्मक, सिद्धांतिक और प्रयोगात्मक अध्ययन किए जाने चाहिए।

इस संदर्भ में, एक संख्यात्मक अध्ययन किया जाता है उच्च तापमान धातुयुक्त ताप बदलने वाली सामग्री (सिलिकॉन) के गलन/कठोरी के दौरान थर्मो-हाइड्रोलिक व्यवहार का अध्ययन करने के लिए। गला हुआ सिलिकॉन में घुमावदार परिसंचार पैटर्न को देखा जाता है, जोकि घुले हुए पारंपरिक उच्च तापमान ताप बदलने वाली सामग्री (सोडियम नाइट्रेट) में घड़ी की दिशा के विपरीत है। सिलिकॉन पर आधारित एलएचएस की ऊष्मा संग्रह प्रतिष्ठा और ऊष्मा संग्रह दरें सोडियम नाइट्रेट (एनएनओ<sub>3</sub>) पर आधारित LHS से काफी अधिक होती हैं। एचटी-एलएचएस प्रणाली के लिए एक उपयुक्त उच्च तापमान धातुयुक्त पीसीएम चुना जाता है, जिसे sCO<sub>2</sub> ब्रेटन चक्र के साथ एकीकृत करने के लिए। रिकंठित स्थिरावस्था मॉडलिंग सीओ<sub>2</sub> ब्रेटन चक्र पर

संघटित स्थानिकीय मॉडलिंग किया जाता है ताकि चरम थर्मोडायनामिक दक्षता पर टरबाइन प्रवेश तापमान का प्रभाव निश्चित किया जा सके। थर्मोडायनामिक दक्षता 700°C पर 50% तक पहुंचती है, जो पारंपरिक रैंकिन चक्र से काफी अधिक है। विद्युतचालितता एक साझी अनुपात 0.75 के लिए थर्मल दक्षता को अधिकतम किया जाता है, एक हवा के तापमान 30°C के लिए। चक्र की दक्षता पर प्रभाव डिस्चार्ज प्रदर्शन का मज़बूत विश्लेषण करने के लिए एक मज़बूत व्याख्यात्मक मॉडल डिमेंशनलेस रूप में विकसित किया गया है और समाधान किया जाता है। पारंपरिक अनायासी नमकों के साथ HT-LHS प्रणालियों के लिए कम ऊष्मा पारंपरिक तकनीकी चुनौती है। अपेक्षाकृत ऊष्मा प्रदर्शन पर गतिशील ऊष्मा संग्रह तकनीकों के व्यक्तिगत और संयुक्त प्रभावों का संख्यात्मक अध्ययन किया जाता है। व्यावसायिक उच्च तापमान अनायासी नमक (NaNO<sub>3</sub> और KNO<sub>3</sub> के इयूटेक्टिक मिश्रण) को एक संरेखित ट्यूब संग्रह प्रणाली में पीसीएम के रूप में मान्यता प्राप्त किया जाता है। उष्मा प्रदर्शन पर संयुक्त प्रभाव को एकल प्रभाव से काफी अधिक बताया गया है। हालांकि, एचटी-एलएचएस प्रणाली के लिए अभिविन्यास और असंतुलन का संयुक्त प्रभाव एचटी-एलएचएस प्रणाली के लिए एक अभिकल्प अवस्था उत्पन्न करता है। (60% NaNO<sub>3</sub>, 40% KNO<sub>3</sub>) इयूटेक्टिक मिश्रण को सामान्य विलयन पद्धति का उपयोग करके बनाया जाता है, और नमूने की थर्मल प्रतिक्रिया का प्रयोगात्मक अध्ययन किया जाता है। एक प्रयोगशाला-मापी विन्यास और प्रयोगात्मक परीक्षण सुविधा डिजाइन की जाती है जो एक संरेखित ट्यूब एचटी-एलएचएस प्रणाली की चार्ज और डिस्चार्ज प्रक्रिया का मिमिक करने के लिए बनाई और विकसित की गई है। इसके अलावा, संख्यात्मक मॉडल के परिणाम प्रयोगात्मक परिणामों के खिलाफ सत्यापित किए जाते हैं। एचटी-एलएचएस प्रणाली की अनिवार्यता को और बेहदी बटरी के साथ तकनीकी-आर्थिक तुलनात्मक अध्ययन द्वारा स्थापित करने के लिए एक तकनीकी-आर्थिक तुलनात्मक अध्ययन किया जाता है जिसमें समान क मता होती है। आपयामी और भारमापी ऊष्मा घनत्व लिथियम-आयन बैटरी से काफी अधिक होते हैं। अवधारणा निम्न चित्र में ग्राफिक रूप में दिखाई जा सकती है।



---

**Declaration by author**

---

This thesis is composed of my original work, and contains no material previously published or written by another person except where due reference has been made in the text. I have clearly stated the contribution of others to jointly authored works that I have included in my thesis.

I have clearly stated the contribution of others to my thesis as a whole, including statistical assistance, survey design, data analysis, significant technical procedures, professional editorial advice, financial support, and any other original research work used or reported in my thesis. The content of my thesis is the result of work I have carried out since the commencement of my higher degree by research candidature and does not include a substantial part of work that has been submitted to qualify for the award of any other degree or diploma in any university or other tertiary institution. I have clearly stated which parts of my thesis, if any, have been submitted to qualify for another award.

I acknowledge that an electronic copy of my thesis must be lodged with the University Library and, subject to the policy and procedures of The University of Queensland, the thesis be made available for research and study in accordance with the Copyright Act 1968 unless a period of embargo has been approved by the Dean of the Graduate School.

I acknowledge that copyright of all material contained in my thesis resides with that material's copyright holder(s). Accordingly, where appropriate I have obtained copyright permission from the copyright holder to reproduce material in this thesis and have sought permission from co-authors for any jointly authored works included in the thesis.

---

## Publications included in the thesis

---

### *International Journal Articles*

1. **A. K. Ray**, D. Rakshit, K. Ravi Kumar, and H. Gurgenci, “Silicon as high-temperature phase-change medium for latent heat storage: A thermo-hydraulic study,” *Sustain. Energy Technol. Assessments*, vol.46, no. September 2020, pp. 101249, 2021.
2. **A. K. Ray**, D. Rakshit, and K. Ravikumar, “High-temperature latent thermal storage system for solar power: Materials, concepts, and challenges,” *Clean.Eng. Technol.*, vol. 4, pp. 100155, 2021.
3. **A. K. Ray**, D. Rakshit, K. Ravikumar, and H. Gurgenci, “A comparative study of high-temperature latent heat storage systems”, *Energies* **2021**, *14*, 68-86.
4. **A. K. Ray**, D. Rakshit, K. Ravikumar, and H. Gurgenci, “Strength-Weakness-Opportunities-Threats-Unusual (SWOT-U) behavior analysis of Silicon as phase change material for high-temperature latent heat storage” *Thermal Science and Engineering Progress* Volume 38, 1, February 2023, 101627.
5. **Alok K.Ray**, Sumer Singh, Dibakar Rakshit, Udayraj, “Comparative study of cooling performance for portable cold storage box using phase change medium” *Thermal Science and Engineering Progress* Volume 27, 1 January 2022, 101146

### *International Conference Articles*

1. **Ray, AK**, Dibakar, R., Kumar, R., Gurgenci, H., a comparative study of melting performance for ultra-high temperature latent storage system. 9th Eur. Conf. Ren. Energy Sys. 21-23 April 2021, Istanbul, Turkey
2. **A. K. Ray**, D. Rakshit, K. Ravikumar, and H. Gurgenci ", A Numerical Investigation of Charging a high-Temperature Latent Heat Storage Unit: A Variable Domain Methodology. Proceedings of the 26th National and 4th International ISHMT-ASTFE Heat and Mass Transfer Conference, December 17-20,2021, IIT Madras, Chennai-600036, Tamil Nadu, India
3. **A. K. Ray**, D. Rakshit, K. Ravikumar, and H. Gurgenci, ‘Thermal performance of eccentric high-temperature latent heat storage system: passive heat transfer enhancement strategy’EuroSun 2022, Kassel, Germany.

4. R. Mochahari, **A.K. Ray** , K. Ravi Kumar and D. Rakshit, "Thermal performance of a supercritical CO<sub>2</sub> based central receiver" THIRD International Conference on Future Technologies in Manufacturing, Automation, Design & Energy, ICoFT 2022, December 14-16, NIT Puducherry.

### ***Book Chapter***

**Ray, AK**, Vashist, S, Joy, J.M, and Rakshit, D, "Comparison Between Ultra-High-Temperature Thermal Battery and Li-Ion Battery", Recent Advances in Fluid Dynamics, Chapter 39, ISBN-978-981-19-3378-3.

---

### **Submitted manuscripts included in this thesis**

---

1. A. K. Ray, D. Rakshit, K. Ravikumar, and H. Gurgenci, "A paradox: Passive heat transfer enhancement strategies enhance thermal performance of high-temperature latent heat storage"
2. A. K. Ray, D. Rakshit, K. Ravikumar, and H. Gurgenci, "Transient discharge performance of high-temperature latent storage system integrated with supercritical CO<sub>2</sub> Brayton cycle: A combined analytical and numerical study"

---

### **Contributions by others to the thesis**

---

#### ***All chapters***

Editorial suggestions were provided by the candidate's supervisors, Prof. Hal Gurgenci, Dr. Dibakar Rakshit, Dr. K. Ravi Kumar and PhD committee members, Prof. Anil Verma, Dr. Anand Veeraragavan and Dr. Kaushik Saha.

---

### **Statement of parts of the thesis submitted to qualify for the award of another degree**

---

No works submitted towards another degree have been included in this thesis.

---

### **Research involving human or animal subjects**

---

No animal or human subjects were involved in this research.

---

## Acknowledgments

---

Despite a long and arduous journey, this course of study has been a formative and essential period of personal development. I take this opportunity to acknowledge and express my profound gratitude to all those who have directly or indirectly been involved in completing my thesis. Without their support and motivation, I could not have achieved this important milestone in my life.

First and foremost, I would like to express my deepest gratitude and most sincere appreciation to my supervisors Prof. Hal Gurgenci, University of Queensland, Dr. Dibakar Rakshit, and Dr. K. Ravi Kumar, Indian Institute of Technology Delhi for giving me such an excellent opportunity to perform the research in the field of thermal energy storage for sustainable energy applications. It has been a learning experience for me, both professionally and personally, through the detailed interactions with supervisors over various activities during my Ph.D.

I wish to express sincere thanks to the members of the research committee, Prof. Anil Verma, Department of Chemical Engineering, IIT Delhi, Dr. Anand Veeraragavan, School of Mechanical and Mining Engineering, UQ, and Dr. Kaushik Saha, Department of Energy Science and Engineering, IITD for providing valuable suggestion at various stages of evaluation of my research work during Ph.D. I thank Prof. Naveen Garg, Dr. Neetu Singh, PIC, UQIIDAR program, Dr. Rajeev Shorey for providing the necessary support during Ph.D.

I am thankful to my senior and fellow lab members -Dr. Ashish Kumar, Dr. Rajat Saxena, Dr. Rupinder Pal, Dr. Anish Malan, Dr. Pranaynil Saikia, Dr. S Sai Saran Yagnamurthy, Ms. Sana Fatima Ali, Sumeet, Mr. Ram, Rahul, Shubham, Mohit, Sagar, Rahul Verma, Mohit Murarka, Suyash, Jibin, Naveen, Rajeev, Santanu, Gaurav and all labmates for helping me and upholding my moral high during tough times of my research work. I would especially thank Mr. Sagar Vasistha for helping with my experimental research work. I would like to thank Mr. Sudeep, and Ms. Vallari for spending quality time in Australia. I thank my hostel mates such as Biswal, Ritesh, Tapo, Sachin, and Sumit. I am also grateful to the UQIDAR administrative staff, IIT Delhi (Mrs. Ramya, Mrs. Ragini), and other student colleagues at IIT Delhi, for extending their support whenever necessary.

I express my heartfelt gratitude towards my parents, family members, and wife for their encouragement and support, without which I couldn't have carried out this work.

At last, thanks to the almighty god who has given me spiritual support and strength to complete this endeavor.

---

**Financial support**

---

This research was supported by an Indian Institute of Technology Delhi Research Scholarship, and a research grant from the UQ-IITD Academy of Research (UQIDAR).

---

**Keywords**

---

Phase change material, High-temperature, latent heat storage, Silicon, Supercritical CO<sub>2</sub> cycle, TIPV, Renewable energy resources

---

**Australian and New Zealand standard research classifications (ANZSRC)**

---

ANZSRC code: 091501, Computational Fluid Dynamics, 40%

ANZSRC code: 091305, Energy Generation, Conversion and Storage Engineering, 40%

ANZSRC code: 091599 Interdisciplinary Engineering not elsewhere classified, 20%

---

**Fields of research classification**

---

FoR code: 4012, Fluid Mechanics and Thermal Engineering, 60%

FoR code: 4099, Other Engineering, 30%

FoR code: 4017, Mechanical Engineering, 10%

## **Contents**

<i>Supervisor Certification</i> .....	i
Abstract .....	ii
Declaration by author.....	vii
Publications included in the thesis .....	viii
Submitted manuscripts included in this thesis .....	ix
Contributions by others to the thesis.....	ix
Statement of parts of the thesis submitted to qualify for the award of another degree.....	ix
Research involving human or animal subjects.....	ix
Acknowledgments.....	x
Financial support.....	xi
Keywords .....	xi
Australian and New Zealand standard research classifications (ANZSRC).....	xi
Fields of research classification .....	xi
List of figures .....	viii

List of tables.....	xiii
Nomenclature.....	xiv
Abbreviations .....	xiv
Greek symbols.....	xiv
Symbols.....	xv
Subscripts .....	xv
1 Introduction .....	1
1.1 Motivation .....	1
1.2 Background .....	3
1.3 Thesis outline .....	6
2 Literature Review and Thesis Objectives.....	8
2.1 Preface.....	8
2.2 Thermal energy storage.....	8
2.2.1 Sensible heat storage.....	9
2.2.2 Latent heat storage .....	10
2.2.3 Thermochemical heat storage (TCHS) .....	11
2.3 Thermal energy storage concepts.....	13
2.4 High-temperature thermal energy storage:.....	14
2.5 High-temperature latent heat storage .....	16
2.5.1 Phase change materials (PCM).....	18
2.5.2 High-temperature metallic PCMs .....	21
2.6 Heat transfer fluid.....	23
2.7 Storage heat exchanger.....	24
2.8 Heat transfer characteristics in high-temperature latent heat storage domain .....	25
2.8.1 Analytical studies.....	25
2.8.2 Experimental studies.....	26
2.8.3 Numerical studies.....	27

2.9	Challenges for high-temperature LHS systems.....	30
2.10	Potential solutions to address challenges .....	30
2.11	Advanced power cycles.....	31
2.11.1	Challenges for advanced sCO <sub>2</sub> cycle [110], [111].....	32
2.12	Literature closure.....	33
3	Thermo-Hydraulic Performance during Melting/Solidification.....	37
3.1	Preface.....	37
3.2	Mathematical and numerical modeling of LHS system.....	37
3.2.1	Effective heat capacity method.....	38
3.2.2	Enthalpy-porosity method:.....	39
3.2.3	Darcy's law source term: .....	40
3.3	Numerical modeling of high-temperature LHS system .....	41
3.3.1	System Description .....	41
3.3.2	Mathematical modelling .....	42
3.4	Results and discussion.....	48
3.4.1	Validation of numerical methodology .....	48
3.4.2	Grid and time independence .....	49
3.5	Thermal performance of Silicon-based LHS System.....	52
3.5.1	Charging of Silicon domain .....	52
3.5.2	Discharging of Silicon Domain .....	56
3.6	Effect of orientation of the domain on charging and discharging performance.....	58
3.7	Anomalous behavior during melting of silicon.....	60
3.8	Energy storage density and energy storage rate .....	63
3.9	Comparison between Effective heat capacity and Enthalpy-Porosity methods.....	65
3.10	Comparison of silicon melting with and without convection .....	65
4	Transient Discharge Performance of High-Temperature Latent Heat Storage System Integrated with sCO <sub>2</sub> Brayton Cycle: A Robust Analytical Model .....	69
4.1	Preface.....	69

4.2	Supercritical Carbondioxide.....	69
4.3	Supercritical CO <sub>2</sub> recompression Brayton cycle.....	70
4.4	Working mechanism of recompression cycle .....	72
4.5	Methodology .....	73
4.6	System description .....	73
4.7	Performance of sCO <sub>2</sub> recompression cycle.....	75
4.8	$\epsilon$ -NTU method to evaluate the effectiveness during discharge process.....	79
4.9	Derivation of an analytical model for discharge process .....	83
4.9.1	Release of heat from PCM.....	84
4.9.2	Combined conduction and convection heat transfer in PCM .....	84
4.9.3	Convective heat transfer from tube to the sCO <sub>2</sub> .....	85
4.9.4	Axial variation of temperature of sCO <sub>2</sub> .....	85
4.9.5	Mathematical formulation of dimensionless variables .....	85
4.9.6	Comparison of the present model with Kantole model: .....	88
4.9.7	Results from the present analytical model .....	89
4.10	Numerical modeling for discharging of the HT-LHS system.....	90
4.10.1	Effective heat capacity model.....	91
4.10.2	System description.....	92
4.10.3	Results and discussion .....	93
5	Thermal Performance of High-Temperature Latent Heat Storage System with Inorganic Phase Change Medium: Effect of Passive Heat Transfer Enhancement Techniques .....	99
5.1	Preface.....	99
5.2	System description .....	99
5.2.1	Physical and computational domain .....	99
5.2.2	Numerical formulation.....	102
5.2.3	Initial and boundary conditions .....	104
5.3	Results and discussion.....	105
5.3.1	Model verification and validation.....	105
5.3.2	Comparison of thermal performance for different inclination angles .....	107
5.3.3	Discharging performance.....	116

5.3.4	Combined effect of orientation and radial eccentricity on discharging performance.	119
5.4	Sensitivity analysis	120
5.4.1	Charging process	121
5.4.2	Discharging process	123
5.5	Latent energy storage and discharge fraction	125
6	Experimental Investigation of Lab-scale High-Temperature LHS Prototype	128
6.1	Preface	128
6.2	Thermal response experiment during heating and cooling of PCM	128
6.3	Sample preparation and characterization	129
6.3.1	Synthesis of HT-PCM	129
6.3.2	Thermo-physical characterization of synthesized PCM	130
6.4	Experimental results and discussion	136
6.4.1	Infrared imaging experiment	136
6.4.2	Isothermal bath experiment	140
6.5	Experimental setup and prototype	144
6.5.1	LHS prototype	145
6.5.2	Gear pump and VFD	147
6.5.3	Heating elements	148
6.5.4	Instrumentation	150
6.5.5	HTF flow rate measurement	151
6.6	Detailed experimental procedure	153
6.6.1	Sample preparation and characterization	153
6.6.2	Charging	153
6.6.3	Preheating the oil	154
6.6.4	Discharging	154
6.7	Results and discussion	154
6.7.1	Temperature variation during charging	155
6.7.2	Charging duration	158
6.7.3	Energy storage	160
6.7.4	Temperature variation during discharging	161

6.7.5	Effect of HTF inlet temperature and flow rate.....	162
6.7.6	Validation of the numerical model with inhouse experimental results.....	165
7	Techno-Economic Performance Comparison between HT-LHS system with Li-ion battery... .....	168
7.1	Preface.....	168
7.2	Methodology .....	168
7.3	Analogy between thermal and electrical parameters.....	170
7.4	System description .....	171
7.5	Numerical formulation .....	173
7.6	Model validation for Li-ion cell analysis .....	174
7.7	Thermal performance comparison .....	175
7.8	Financial Evaluation.....	182
7.8.1	Levelized cost of electricity .....	182
7.8.2	Estimation of levelized cost of electricity.....	189
7.8.3	Sensitivity analysis.....	190
8	Conclusions and Scope for Future Work.....	194
8.1	Preface.....	194
8.2	Major outcomes.....	194
8.3	Scope for future work.....	195
A	Appendix A: Variable Domain Numerical Methodology .....	197
A.1	Preface.....	197
A.2	Numerical implementation of variable domain methodology.....	199
A.3	System description .....	200
A.4	Results and discussion.....	202
A.4.1	Model Verification and Validation.....	202
A.4.2	Temperature distribution with velocity vectors for NaNO <sub>3</sub> domain.....	204
A.4.3	Temporal evolution of melting interface for NaNO <sub>3</sub> domain.....	204

A.4.4	Stefan’s heat balance at phase change interface during melting in NaNO <sub>3</sub> domain	205
A.5	Melting in Silicon domain.....	206
A.5.1	Temperature distribution with velocity vectors for silicon domain.....	207
A.5.2	Temporal evolution of melting interface for Silicon domain .....	207
A.6	Closure: .....	208
B	Appendix B: Suitability of Silicon based HT-LHS System for Integration with TIPV System	
	.....	209
B.1	Preface.....	209
B.2	Working principle of Thermionic photovoltaic system .....	209
B.3	Governing Equations for idealized TIPV:.....	210
B.4	Bandgap calculation for silicon.....	212
B.5	Workfunction analysis of a Thermionic (TI) device.....	214
B.6	Closure: .....	216
C	Appendix C: Uncertainty and Repeatability in Experiments .....	217
C.1	Uncertainty analysis .....	217
C.2	Repeatability in experiments.....	220
D.	Appendix D:Temperature Dependent Properties of PCM and HTF	
	.....	222
	References.....	224

---

## List of figures

---

Figure 1-1: Energy storage technologies .....	2
Figure 1-2: Three processes of TES. (a) Charging (Heat absorption), (b) Standby (Heat storage), and (c) Discharging (Heat release) [11].....	3
Figure 1-3: Different strategies for HT-LHS integration. (a) CST system, and (b) TIPV system .	5
Figure 2-1: Classification of thermal storage mechanism .....	9
Figure 2-2: Classification of SHS mediums .....	10
Figure 2-3: Energy stored and released in a medium during melting and solidification.....	11
Figure 2-4: Classification of TCHS systems .....	12
Figure 2-5: Different types of thermal energy storage concepts.....	14
Figure 2-6: Thermal efficiency of technologies as function of temperature .....	15
Figure 2-7: TES systems based on operating temperature.....	16
Figure 2-8: Classification of PCMs based on the operating temperature range .....	17
Figure 2-9: Classification of solid-liquid phase change materials.....	18
Figure 2-10: Application domains of PCM .....	21
Figure 2-11: Operating temperature range of HTFs [61].....	23
Figure 2-12: Classification of different performance enhancement techniques .....	31
Figure 2-13: Classification of advanced power cycles .....	32
Figure 2-14: Flow chart of the methodology under the present study .....	36
Figure 3-1: Graphical representation of effective heat capacity method.....	39
Figure 3-2: Graphical representation of enthalpy-porosity method.....	40
Figure 3-3: Numerical model. (a) Computational domain, and (b) Discretized geometry.....	42
Figure 3-4: Modified specific heat. (a) Silicon and (b) NaNO <sub>3</sub> .....	45
Figure 3-5: Liquid fraction as a function of temperature. (a) Silicon, and (b) NaNO <sub>3</sub> .....	46
Figure 3-6: Validation of the current numerical formulation .....	49
Figure 3-7: Numerical model verification. (a) Grid independence test, and (b)Time independence test.....	51
Figure 3-8: Melting of silicon at different instants with $q'' = 7500 \text{ W/m}^2$ . (a) Liquid fraction (b)Temperature distribution, (c) Streamlines, and (d) Velocity distribution.....	53
Figure 3-9: Effect of heat flux on charging of domain .....	55
Figure 3-10: Effect of heat flux on charging efficiency with silicon system.....	56
Figure 3-11: Temporal distribution of temperature and solid fraction. (a) Temperature with velocity vectors and (b) Solid fraction.....	57
Figure 3-12: Influence of heat flux on discharge performance for silicon domain .....	58
Figure 3-13: Influence of orientation on thermal performance for silicon. (a) Charging, and (b) Discharging.....	60
Figure 3-14: Melting of NaNO <sub>3</sub> with $q'' = 7500 \text{ W/m}^2$ . (a) Liquid fraction, (b) Temperature distribution, (c) Velocity distributions, and (d) Streamlines.....	62
Figure 3-15: Temporal evolution of melting interface in HT-LHS system. (a) Silicon domain and (b) NaNO <sub>3</sub> domain .....	63
Figure 3-16: Comparison of energy storage rate and density during charging of silicon and NaNO <sub>3</sub> domain.....	64
Figure 3-17: Comparison between EHC and E-P methods for silicon melting.....	65

Figure 3-18: Melting of silicon without and with convection. (a) Only conduction, and (b) Combined conduction and convection (t = 4 hrs).....	67
Figure 3-19: Comparison between pure conduction and combined conduction /convection model for silicon .....	67
Figure 4-1: Phase diagram of carbon dioxide [121] .....	70
Figure 4-2: (a) Coupling of high-temperature latent heat storage (LHS) with sCO <sub>2</sub> recompression cycle and (b)T-s diagram of recompression cycle .....	72
Figure 4-3:Schematic of shell and multitube phase change heat exchanger .....	74
Figure 4-4: Effect of turbine inlet temperatures on thermal efficiency and net power output of sCO <sub>2</sub> recompression cycle (Thermal efficiency , Power output ), Compressor inlet temperature = 45°C .....	77
Figure 4-5: Effect of mass flow rate on efficiency and power output of sCO <sub>2</sub> cycle (T <sub>turbine</sub> = 700°C and SR= 0.75) .....	78
Figure 4-6: Sensitivity analysis for the cycle efficiency.....	79
Figure 4-7: (a) Simplified model with one tube, and (b)Thermal resistance circuit of the simplified model.....	80
Figure 4-8:Variation of average effectiveness with ratio of mass flow rate to the area of LHS ..	82
Figure 4-9: Variation of average effectiveness of LHS with V/A <sub>s</sub> for different Reynold's number .....	82
Figure 4-10: Flow of thermal energy from molten PCM to sCO <sub>2</sub> .....	83
Figure 4-11: Comparison between present and Kantole model.....	88
Figure 4-12: Different steps to evaluate the thermal performance of high-temperature LHS from the analytical model .....	89
Figure 4-13: (a) Effective heat capacity of PCM during phase change, and (b) Melting fraction distribution as a function of temperature .....	91
Figure 4-14: Cross-sections of the geometry. (a) Physical domain and (b) Computational domain in magnified view (top-right quarter) .....	92
Figure 4-15: 3D geometry of the computational domain. (a) Computational domain and (b) Discretized geometry .....	93
Figure 4-16: Average liquid fraction during melting of PCM.....	94
Figure 4-17: Effect of the unit cell orientation on discharge duration.....	95
Figure 4-18: Solid fraction contour during discharging of high-temperature LHS .....	97
Figure 4-19: Temperature contour during discharging of high-temperature LHS .....	97
Figure 5-1: Physical and computational domain of the LHS system. (a) $\theta = 0^\circ$ , (b) $\theta = 30^\circ$ , (c) $\theta = 60^\circ$ and (d) $\theta = 90^\circ$ .....	101
Figure 5-2: Flowchart of enthalpy-porosity numerical algorithm .....	104
Figure 5-3:Verification of the model (a) Grid independence test and (b) Time independence test of the 3D computational domain ( $\theta = 0^\circ$ , T <sub>in, HTF</sub> =525 K, Q <sub>in,HTF</sub> = 0.5 LPM) .....	106
Figure 5-4: Schematic of discretized computational domain (a) Cross section of the 3D geometry for $\theta = 0^\circ$ , $30^\circ$ and $60^\circ$ , and (b) 2D axisymmetric domain for $\theta = 90^\circ$ .....	106
Figure 5-5: Comparison of the present numerical model with existing experimental and numerical results .....	107

Figure 5-6: Temporal variation of liquid fraction and average temperature of PCM domain for LHS system of $\theta = 0^\circ$ at a cross-section of $z = 0.5$ m. (a) Liquid fraction contour and (b) Average PCM temperature (K) contour .....	109
Figure 5-7: Temporal variation of liquid fraction and the average temperature of PCM domain for LHS system for $\theta = 90^\circ$ at a cross-section of $z = 0.5$ m. (a) Liquid fraction contour and (b) PCM temperature contour .....	111
Figure 5-8: Temporal variation of average liquid fraction and temperature of PCM domain. (a) liquid fraction and (b) PCM temperature.....	112
Figure 5-9: Cross section of horizontal domains with eccentricity in horizontal and vertical directions.....	113
Figure 5-10: Liquid fraction variation with Fourier number at different eccentricity ratios ( $e_r$ )	114
Figure 5-11: Variation of effectiveness with eccentricity ratio for the horizontal domain ( $\theta = 0^\circ$ ) .....	115
Figure 5-12: Liquid fraction and temperature contours of $\theta = 0^\circ$ orientation during discharging (a) Liquid fraction and (b) Temperature.....	117
Figure 5-13: Liquid fraction and temperature contours for $\theta = 90^\circ$ orientation during discharging. (a) Liquid fraction and (b) Temperature .....	118
Figure 5-14: Temporal variation of average liquid fraction and temperature of PCM domain during the discharge process (LF = Liquid fraction).....	118
Figure 5-15: Effect of vertical eccentricity on discharging duration for $\theta = 0^\circ$ domain.....	120
Figure 5-16: Temporal variation of Liquid fraction as a function of Rayleigh number and Stefan number .....	122
Figure 5-17: Temporal variation of liquid fraction as a function of Reynold's number .....	123
Figure 5-18: Temporal variation of liquid fraction as a function of Reynold's number .....	124
Figure 5-19: Temporal variation of liquid fraction as a function of Rayleigh number .....	125
Figure 5-20: Latent Storage and discharge fraction as function of inclination angle. (a) LSF, and (b) LDF .....	126
Figure 6-1: Methodology followed to observe thermal response of the HT-PCM.....	129
Figure 6-2: Different steps for preparation of HT-PCM (Eutectic mixture). (a) Solubility of $\text{NaNO}_3$ and $\text{KNO}_3$ in water concerning temperature, (b) Weighing balance to measure specific weight of $\text{NaNO}_3$ and $\text{KNO}_3$ , (c) Hot plate magnetic stirrer for uniform mixture, and (d) Eutectic mixture after evaporation of water .....	130
Figure 6-3: Pictorial images of different components of DSC. (a) DSC system, (b) Crimping machine, (c) DSC pan and dies, and (d) DSC cell.....	132
Figure 6-4: DSC analysis of synthesized HT-PCM. (a) Melting and (b) Solidification curve...	133
Figure 6-5: TGA analysis of synthesized HT-PCM .....	133
Figure 6-6: XRD analysis of synthesized PCM (Eutectic mixture).....	135
Figure 6-7: SEM images of the synthesized PCM before heating. (a) 300X, (b) 800X, (c) 1500X, and (d) 4000X .....	136
Figure 6-8: Experimental setup for IR imaging experiment.....	137
Figure 6-9: Spatiotemporal variation of the surface temperature of PCM during heating .....	138
Figure 6-10: Spatiotemporal variation of the surface temperature of PCM during cooling.....	139
Figure 6-11: Experimental setup for heat heating-cooling of HT-PCM in isothermal bath.....	140

Figure 6-12: Temporal evolution of melting/solidification of PCM. (a) Melting, and (b) Solidification .....	141
Figure 6-13: Transient variation of PCM temperature during heating/cooling in isothermal bath. (a) Heating curve, and (b) Cooling curve .....	142
Figure 6-14: Cooling of HT-PCM in two isothermal baths .....	143
Figure 6-15: Schematic of experimental test facility .....	144
Figure 6-16: Cross-section of the LHS prototype. (a) Charging with heat flux, and (b) Charging with HTF .....	145
Figure 6-17: Empty test section (concentric tube heat exchanger with inlet and outlet hopper)	147
Figure 6-18: Photographs of gear pump and VFD .....	148
Figure 6-19: Heating elements. (a) Ceramic band heater with insulation and (b) Nichrome wire .....	149
Figure 6-20: (a) Panel board (PID controller), and (b) Autotransformer (variac) .....	150
Figure 6-21: Photograph of the NI data logger .....	150
Figure 6-22: Photographs of thermocouple calibrator and K-type thermocouple with a probe	151
Figure 6-23: Photograph of turbine flow meter .....	152
Figure 6-24: (a) Photograph of energy meter, and (b) Pressure transducer .....	152
Figure 6-25: Experimental test facility .....	153
Figure 6-26: Position of thermocouples in LHS prototype during charging for two configurations. (a) Horizontal ( $\theta = 0^\circ$ ) and (b) Vertical ( $\theta = 90^\circ$ ) .....	154
Figure 6-27: (a) Local temperature variation for $q = 1000 \text{ W/m}^2$ and (b) Average liquid fraction during charging .....	156
Figure 6-28: Local temperature variation during charging at different electric flux (a) Thermocouple locations A, B and C (b) Thermocouple locations D, E, and F .....	157
Figure 6-29: Local temperature variation during charging for vertically oriented LHS .....	158
Figure 6-30: Local melting fraction variation. (a) $q = 1000 \text{ W/m}^2$ , and (b) $q = 2000 \text{ W/m}^2$ .....	160
Figure 6-31: Total energy stored in LHS prototype .....	161
Figure 6-32: Local variation of temperature during discharging .....	162
Figure 6-33: Local variation of temperature during discharging. (a) Inlet temperature of HTF = $30^\circ\text{C}$ , and (b) Inlet flow rate = 5 LPM .....	164
Figure 6-34: Temporal evolution of liquid fraction during discharging .....	165
Figure 6-35: Validation of numerical prediction with experimental results. (a) melting fraction during charging, and (b) average temperature during discharging .....	166
Figure 7-1: Flow chart of the methodology. (a) Storage of electrical energy using both technologies and (b) Thermo-economic performance comparison Schematic of the flowchart for thermo-economic performance comparison .....	170
Figure 7-2: Dimensions of the two selected systems. (a) Li-ion cell, and (b) Thermal cell .....	173
Figure 7-3: A comparison of measured and simulated voltages using the NTGK model .....	175
Figure 7-4: Transient variation of melting fraction in thermal cell. (a) Silicon, and (b) AlSi <sub>12</sub> ..	176
Figure 7-5: Transient variation of average temperature. (a) Silicon, and (b) AlSi <sub>12</sub> .....	177
Figure 7-6: Temporal variation of cell voltage .....	178
Figure 7-7: Temporal variation of charged capacity .....	179
Figure 7-8: Temporal variation of cell voltage .....	180

Figure 7-9: Temporal variation of discharged capacity .....	181
Figure 7-10: Sensitivity analysis for LCoE . (a) Thermal battery and (b) Li-ion Battery Energy storage system.....	192
Figure A-1: Numerical implementation of VDM .....	199
Figure A-2: Computational and discretized domain. (a) Computational domain, and (b) discretized domain at different instants.....	201
Figure A-3: Independence test. (a) Initial layer thickness independency and (b) Grid independency test .....	203
Figure A-4: Interface position during melting of tin. (a) Numerical results from Hannoun et al., and (b) Results from present methodology .....	203
Figure A-5: Temperature distribution in molten PCM. (a) $t = 1$ h, (b) $t = 2$ h, (c) $t = 4$ h, and (d) $t = 8$ h .....	204
Figure A-6: Temporal evolution of $\text{NaNO}_3$ melting interface at an interval of 0.5 h.....	205
Figure A-7: Stefan's energy balance at $\text{NaNO}_3$ phase change interface .....	206
Figure A-8: Temperature distribution in molten silicon . (a) $t = 1/12$ h, (b) $t = 1/4$ h, (c) $t = 1/2$ h, (d) $t = 1$ h, (e) 1.5 h, and (f) 2 h. ....	207
Figure A-9: Temporal evolution of silicon melting interface.....	208
Figure B-1: Bandgap diagram of the two-terminal hybrid thermionic-photovoltaic (TIPV) converter [147].....	210
Figure B-2: Bandgap variation as a function of temperature.....	213
Figure B-3: Planck's curve at melting temperature of Silicon .....	214
Figure B-4: Variation of power density and efficiency of TI device as a function of emitter temperature .....	216
Figure C-1: Repeatability assessment of charging experiment.....	220
Figure .C-2: Repeatability assessment of discharging experiment.....	221

---

## List of tables

---

Table 2-1: Comparison between SHS, LHS, and TCHS .....	12
Table 2-2: Properties of PCM and their effect on HT-LHS system .....	19
Table 3-1. Properties of silicon and $\text{NaNO}_3$ .....	42
Table 3-2. Initial and boundary conditions during melting and solidification .....	43
Table 3-3. Mesh statistics and quality.....	50
Table 3-4. Fixed operating parameters for both LHS systems .....	60
Table 4-1. Thermophysical properties of $\text{Cu}_{57}\text{Si}_{27}\text{Mg}_{16}$ [123].....	74
Table 4-2. Thermophysical properties of $\text{sCO}_2$ [124].....	75
Table 4-3: Parameters considered to assess the thermal performance of $\text{sCO}_2$ cycle [111].....	76
Table 4-4. Initial and boundary conditions for the model .....	87
Table 4-5: Variables obtained after solving the dimensionless equation .....	90
Table 4-6. Initial and boundary conditions during discharging.....	93
Table 5-1: Quantitative demonstration of individual and combined effect of eccentricity and orientation .....	114
Table 5-2: Discharging duration for different orientations of LHS domain.....	119
Table 5-3: Analyzed cases .....	120
Table 6-1. Dimensions of LHS prototype.....	146
Table 6-2. Specifications of the heating elements .....	149
Table 7-1. Thermal-electrical circuit analogy.....	170
Table 7-2. Specification of the selected Li-ion cell .....	171
Table 7-3:Charging time for Li-ion battery under different C-rating.....	178
Table 7-4. Discharging time for Li-ion battery under different C-rating .....	180
Table 7-5: Comparison between thermal storage and Li-ion battery .....	181
Table 7-6. Capital cost calculation for li-ion BESS.....	184
Table 7-7. Financial parameters for Li-ion BESS [139].....	186
Table 7-8.Cost contributors of the LHS system.....	188
Table 7-9. Financial parameters for LCoE calculation.....	189
Table 7-10.Comparison between TES and ECS .....	192
Table A-1. Comparison between FDM and VDM.....	197
Table A-2.Initial and boundary conditions .....	201
Table D.1. Temperature dependent PCM properties .....	222
Table D.2. Temperature dependent HTF (Therminol VP1) properties .....	222
Table D.3. Temperature dependent HTF (Hi-Tech Therm 60) properties .....	223

---

## Nomenclature

---

### Abbreviations

AR	Aspect ratio	NTU	Number of transfer units
CCW	Counterclockwise	Nu	Nusselt number
CST	Concentrated solar thermal	PCM	Phase change medium
DSC	Differential scanning calorimetry	Pr	Prandtl number
DSG	Direct steam generation	PV	Photovoltaic
EHC	Effective heat capacity	Ra	Rayleigh number
Fo	Fourier number	Re	Reynold's number
Gr	Grashoff number	RER	Renewable energy resources
HTF	Heat transfer fluid	sCO <sub>2</sub>	Supercritical carbon dioxide
HT	High temperature	SEM	Scanning electron microscope
lpm	Liter per minute	SHS	Sensible heat storage
LCoE	Levelized cost of energy	Ste	Stefan number
LDF	Latent discharge fraction	TCHS	Thermochemical heat storage
LHS	Latent heat storage	TES	Thermal energy storage
LSF	Latent storage fraction	TGA	Thermo-gravimetric analysis
MF	Melting fraction	TIPV	Thermionic photovoltaic

### Greek symbols

$\alpha$ (m <sup>2</sup> /s)	Thermal diffusivity	$\Phi$ (eV)	Workfunction
$\beta$	Liquid fraction/melt fraction	$\lambda$ ( $\mu$ m)	Wavelength
$\delta$	Solid fraction	$\mu$ (Pa.s)	Dynamic viscosity
$\vec{\nabla}$	Divergence	$\rho$ (kg/m <sup>3</sup> )	Density
$\varepsilon$	effectiveness	$\nabla$	Gradient
$\eta$	efficiency	$\theta$ (°)	Inclination

## Symbols

A (kg/s)	Mushy zone constant	$\Delta H_r$ (kJ/mol)	Enthalpy of reaction
$a_r$	Percentage of conversion	$j_{ECH}$	Volumetric current transfer rate
$A_s$ (m <sup>2</sup> )	Surface area	$k$ (W/mK)	Thermal conductivity
$c_p$ (kJ/kgK)	Specific heat capacity	$K$ (D)	Permeability
$D(T)$	Darcy term	$k_T$ (1/K)	Coefficient of thermal expansion
$e$ (mm)	eccentricity	$q''$ (W/m <sup>2</sup> )	Heat flux
$E$ (kJ)	Energy stored/released	$S$	Shape factor
$f$	Friction factor	$\dot{q}$ (kJ/m <sup>3</sup> )	Heat generation rate
$flc2hs$	Heavyside function	$S_{dis}$ (kJ/m <sup>3</sup> )	Energy dissipation
$h$ (kJ)	Sensible enthalpy	$S(\beta)$ (kg/s)	Source term in N-S equation
$h_{sl}$ (kJ/kg)	Latent heat of fusion/solidification	$U$ (W/m <sup>2</sup> K)	Overall heat transfer coefficient
$H$ (kJ)	Total enthalpy	$U$ (V)	Open circuit voltage

## Subscripts

$T_i$ (K)	Initial temperature	$\epsilon_{avg}$	Average effectiveness
$T_f$ (K)	Final temperature	$e_x$ (mm)	Horizontal eccentricity
$T_s/T_{Solid}$ (K)	Solidification temperature	$e_y$ (mm)	Vertical eccentricity
$T_l/T_{liq}$ (K)	Liquidus temperature	$\Phi_e$ (eV)	Emitter work function
$C_{eff}$ (J/kgK)	Effective heat capacity	$\Phi_c$ (eV)	Collector work function
$\eta_{Tur}$	Turbine efficiency	$Q_{el}$ (kJ)	Energy transfer through electron
$\eta_{comp}$	Compressor efficiency	$Q_{ph}$ (kJ)	Energy transfer through photon
$\epsilon_{Recup}$	Recuperator effectiveness	$\rho_{mod}$ (kg/m <sup>3</sup> )	Modified density
$T_m$ (K)	Melting point	$E_{discharge}$ (kJ)	Energy discharged
$d_o$ (mm)	Outer diameter	$d_i$ (mm)	Inner diameter
$e_r$ (mm)	Radial eccentricity	$d_m$ (mm)	Mean diameter